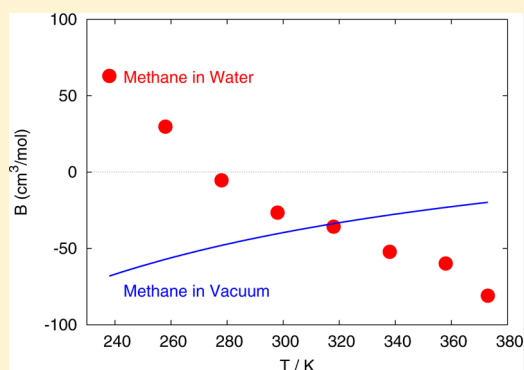


Osmotic Second Virial Coefficient of Methane in Water

K. Koga

Department of Chemistry, Faculty of Science, Okayama University, Okayama 700-8530, Japan

ABSTRACT: A correlation-function-based scheme is proposed for calculating the osmotic second virial coefficient B for solutes that dissolve very little in a solvent. The short-distance contribution to B , a volume integral of the solute–solute pair correlation function $h(r)$ from 0 to some finite distance r_c , is evaluated with $h(r)$ obtained by molecular simulation. The remaining contribution to B from r_c to ∞ is calculated with an asymptotic form of $h(r)$ (Evans, R.; et al. *J. Chem. Phys.* **1994**, *100*, 591). It is shown here that B for a model system of methane in water is obtained accurately in the temperature range between 238 and 373 K at 1 bar, with a result that B is a monotonically decreasing function of temperature, and the hydrophobic interaction between methane molecules measured by B is repulsive ($B > 0$) in supercooled water, virtually null ($B \approx 0$) at around 0 °C, and attractive ($B < 0$) at higher temperatures. It is also remarked that a nearly linear relation holds between B and the first-peak height of the solute–solute radial distribution function.



I. INTRODUCTION

The term “hydrophobic effect” often indicates that nonpolar molecules dissolve very little in water and once in the very dilute solution they attract each other strongly. It is, however, very difficult to verify the latter by experiment, precisely because they are so dilute in water that their spatial correlation cannot be measured. There are pioneering and recent theoretical developments on the hydrophobic interactions.^{1–14} It has been pointed out that the low solubility of a hydrophobic solute in water does not necessarily imply existence of strong attractive pairwise interactions.^{2,3,7} The osmotic second virial coefficient B is an important measure of the strength of the effective pair interaction between solute molecules in the limit of infinite dilution: it is related to the potential $w(r)$ of mean force:^{18,19}

$$B = -\frac{1}{2} \int (e^{-w(r)/kT} - 1) d\tau \quad (1)$$

where k is Boltzmann’s constant, T is the temperature, and the integral is over all space with the volume element $d\tau$. The potential $w(r)$ is related to the solute–solute pair correlation function $h(r)$ by $w(r) = -kT \ln[h(r) + 1]$, and so

$$B = -\frac{1}{2} \int h(r) d\tau = -2\pi \int_0^\infty h(r)r^2 dr \quad (2)$$

which is one of the Kirkwood–Buff integrals at infinite dilution. Both $w(r)$ and $h(r)$ depend on the choice of molecular “centers” from which the distance r is measured; the integrals (eqs 1 and 2) are invariant to the choice.²⁰ Expression 1 for B is a generalization of that for the second virial coefficient B_{gas} of gases, because in vacuum $w(r)$ is just the pair potential $\phi(r)$ and eq 1 is then the standard formula for B_{gas} . Comparison of the osmotic B for a solute with the gas-phase B_{gas} would then give a

quantitative answer to the question whether the solute molecules attract more strongly in the solution than in vacuum.

There are a number of measurements of B for aqueous solutions of proteins—large, complex molecules—either by the osmotic pressure or light scattering; but the corresponding direct measurements of B for small hydrophobic solutes are much more difficult, if not impossible. Previous studies have evaluated B for small alkanes or inert gases, either from the pair correlation function obtained by computer simulation,^{2,4,7,20} from thermodynamic relations with input of solubility measurements,^{2,3,8,15} or from analytic equations of state.^{16,17} However, the estimates of B for methane at room temperature, for example, differ among different methods to the extent that one cannot determine its sign,^{2,7,15} and the temperature dependence of B has not been determined for many solutes. A main purpose of this paper is to calculate the osmotic second virial coefficient for methane in water as accurately as possible. To that end, we propose a correlation-function-based scheme for calculating B , which evaluates both the short-range and long-range contributions to B . We then compare the magnitude and temperature dependence with those for B_{gas} and those for B for a model solute that has a short-range, repulsive pair potential. We also seek for a simple relation between B and some other quantity that can be obtained with less computational effort.

II. MODEL AND SCHEME

Molecular dynamics simulations of an aqueous solution of methane have been performed with the following model system. The model water is the TIP4P/2005²¹ with the LJ potential truncated at 9 Å; the long-range Coulomb interaction

Received: August 26, 2013

Revised: September 17, 2013

Published: September 19, 2013

is treated by the Ewald sum with a real-space cutoff of 9 Å. The pair potential for methane is of the united-atom Lennard-Jones (LJ) with the energy and size parameters²² $\epsilon_2 = 1.2301$ kJ/mol and $\sigma_2 = 3.73$ Å, which gives accurate $B_{\text{gas}}(T)$ for methane. The pair potential for methane–water interactions is the LJ function with the parameter set proposed by Docherty et al.:²³ $\epsilon_{12} = 1.043$ kJ/mol and $\sigma_{12} = 3.4445$ Å. The potential models for water–water and methane–water interactions employed here reproduce with remarkable accuracy the density of pure water²¹ and the solubility of methane in water over a wide temperature range at 1 bar.²³ It is also known that for a given water model the solvent polarizability has a smaller effect on the methane–methane correlation function than does the structure of the water model.²⁴ The model system employed here may therefore be one of the best to reproduce equilibrium properties of an aqueous solution of methane.

The scheme for calculating B from the correlation-function integral (eq 2) consists of three steps. The first is to calculate with greatest possible accuracy the solute–solute radial distribution function $g(r) [=h(r) + 1]$ by performing molecular dynamics simulations of the dilute solution. For the integral $\int h(r) dr$ to converge, it is necessary that $g(r) \rightarrow 1$ as $r \rightarrow \infty$. For a closed system, however, the radial distribution function $g_N(r)$ converges to $1 - c/N < 1$, with N being the number of solute particles and c an intensive quantity, as derived by Lebowitz and Percus²⁵ and recalled by Kežić and Perera.²⁶ If the system size is sufficiently large and the solute–solute pair potential is of short-range, then $g_N(r)$ oscillates around a constant value for r less than half the dimension of the cell. The constant c is then determined by the condition

$$\int_0^R \left[\frac{g_N(r)}{1 - c/N} - 1 \right] r^2 dr$$

not be diverging with increasing the upper limit R of the integral. The resulting $g_N(r)/[1 - c/N]$ is the $g(r)$ with the correct asymptote 1. Furthermore, it must be confirmed that $g(r)$ is independent of the concentration of the solute molecules and of the system size. Then, one may assume that $g(r)$ is essentially the same as that at infinite dilution, which is required for calculating B . There is a simple, efficient trick of minimizing the effect of finite concentrations of solute particles on $g(r)$, as we employed in this work: that is to replace the LJ potential $\phi(r)$ for the methane–methane interaction by the repulsive Weeks–Chandler–Andersen (WCA) potential $\phi_{\text{WCA}}(r)$ in the simulation, while keeping all the other potentials the same. Because the purely repulsive WCA particles have less tendency to aggregate into a cluster in the solution, one can obtain the concentration-independent $g_{\text{WCA}}(r)$ at concentrations higher than those required for the original system. Once the infinite-dilution limit of $g_{\text{WCA}}(r)$ is obtained, one has the corresponding $g(r)$

$$g(r) = g_{\text{WCA}}(r) e^{-\phi_{\text{attr}}(r)/kT} \quad (3)$$

where $\phi_{\text{attr}}(r) = \phi(r) - \phi_{\text{WCA}}(r)$, the attractive part of the WCA potential.

In the second step, with $h(r) = g(r) - 1$ now obtained, one calculates the short-range contribution to B from the finite range $0 < r < r_c$:

$$B_{\text{short}}(r_c) = -2\pi \int_0^{r_c} h(r) r^2 dr \quad (4)$$

In Figure 1, B_{short} at 298 K and 1 bar is plotted as a function of r_c the upper limit of the integral. Note that, even for r_c greater than 15 Å, B_{short} still oscillates.

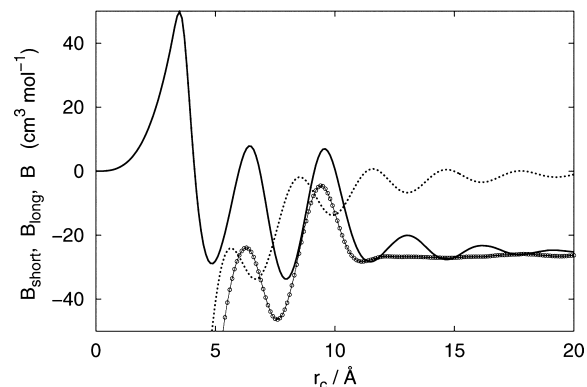


Figure 1. The short-range and long-range contributions to B : $B_{\text{short}}(r_c)$ (solid line), $B_{\text{long}}(r_c)$ (dotted line), and the sum (solid line with dots). $T = 298$ K and $p = 1$ bar.

The third step is to calculate the long-range contribution to B . Although $h(r)$ is obtained by molecular simulation up to a fairly large distance r_c with great accuracy, $h(r)$ beyond $r = r_c$ is required for calculating the long-range contribution

$$B_{\text{long}}(r_c) = -2\pi \int_{r_c}^{\infty} h(r) r^2 dr \quad (5)$$

What is proposed here is to use an exact asymptotic expression for the pair correlation function between particles with short-range interactions derived by Evans et al.²⁷

$$r h_{\text{WCA}}(r) = A e^{-r/\xi} \cos(ar - \theta) \quad (6)$$

where the subscript WCA anticipates an application to the WCA solute particles, although eq 6 is valid for any short-ranged pair potential. The parameters A , ξ , a , and θ are determined by fitting eq 6 to the numerical data for the WCA solute particles in water obtained in the first step. The range of r for fitting must be where r is large enough for the asymptotic form (eq 6) to be valid and the numerical data are accurate enough for fitting of $r h_{\text{WCA}}(r)$. In practice, we have chosen the range of r between the third and fifth minima in $h_{\text{WCA}}(r)$. Figure 2 shows $h_{\text{WCA}}(r)$ obtained from simulation and the asymptotic form $(A/r) e^{-r/\xi} \cos(ar - \theta)$ with the parameters fitted to the data. The fit is very good from $r = 12$ Å, the distance of the third minimum in h_{WCA} . Oscillations in h_{WCA} are visible up to 20 Å, which manifests itself in B_{short} in Figure 1.

With eq 6 and the exact relation between $h(r)$ and $h_{\text{WCA}}(r)$ (an analogue of eq 3), the long-range contribution (eq 5) to B is numerically calculated. An example of $B_{\text{long}}(r_c)$ is shown in Figure 1 (the dotted line). Since the asymptotic form (eq 6) for $h_{\text{WCA}}(r)$ is only valid for large r (in practice, $r \gtrsim 12$ Å), $B_{\text{long}}(r_c)$ is valid only for large r_c . It may be emphasized here that $B_{\text{long}}(r_c)$ includes the contribution of the direct pair potential $\phi(r)$, which decays as $1/r^6$ at large r , and that of the solvent-induced potential, both from the infinite range $r_c < r < \infty$.

Finally, one has the full integral (eq 2)

$$B = B_{\text{short}}(r_c) + B_{\text{long}}(r_c) \quad (7)$$

This B should be independent of r_c if $B_{\text{long}}(r_c)$ is accurately evaluated from eq 6. Figure 1 shows $B_{\text{short}}(r_c) + B_{\text{long}}(r_c)$ as a

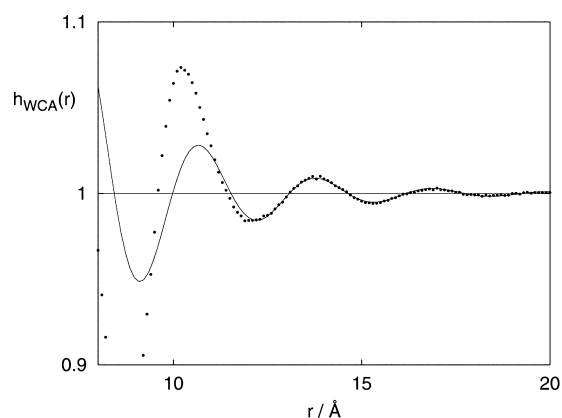


Figure 2. The pair correlation function $h_{\text{WCA}}(r)$ for the WCA solutes in water obtained by simulation (dots) and the exact asymptotic form (solid line) (see eq 6). $T = 298$ K and $p = 1$ bar.

function of r_c . One can see that, for $r_c \gtrsim 12$ Å, the sum is nearly constant, while each of the two terms still oscillates with increasing r_c . The sum at any r_c in this range may therefore be taken to be the B we wished to calculate.

We performed isobaric–isothermal molecular dynamics simulations of dilute aqueous solutions of methane at eight thermodynamic states along the isobar of 1 bar between 238 and 373 K, as listed in Table 1: two supercooled states (238

Table 1. The Osmotic Second Virial Coefficient B for the Model Aqueous Solution of Methane and the First Peak Height $g(r_1)$ of the Solute–Solute Radial Distribution Function at $r_1 = 3.9$ Å^a

T (K)	B (cm ³ /mol)	$g(r_1)$
238	63.0	1.64
258	29.7	2.08
278	−5.4	2.44
298	−26.6	2.86
318	−35.7	3.13
338	−52.2	3.35
358	−59.9	3.47
373	−81.0	3.61

^aThe error bars in B are the same as those in Figure 4.

and 258 K) and six stable states from 278 K to the boiling point of water. The simulations were done with GROMACS (GRONingen MACHine for Chemical Simulations)²⁸ and the model potentials described above. The pressure–temperature control was implemented by the Nosé–Hoover method. The system size and the solute concentration were carefully chosen from preliminary simulations so that the solute–solute $g(r)$ is unchanged as the size is increased or the concentration is decreased: the numbers of solvent and solute molecules are, respectively, $N_w = 4000$ and $N = 48$. This concentration is higher than those of methane in liquid water with its vapor at 1 bar, but we have confirmed that $g(r)$ is independent of N if $N \leq 80$. The net simulation length for production runs is 400 ns at 238 K and 100 ns at higher temperatures.

III. RESULTS AND DISCUSSION

In Figure 3, plotted are $g(r)$ and $w(r)/kT$ for methane pairs in water at the eight different temperatures. These are the input data to calculate B_{short} . It is clearly seen that the higher the temperature, the higher the first peak in $g(r)$ and the lower the first minimum in $w(r)$ (the position r_1 of the first peak remains to be 3.9 Å). See Table 1 for the values of $g(r_1)$. This temperature dependence of $g(r_1)$, or that of the potential $w(r_1)$ of mean force, has already been reported with different models and methods;^{5,6,9–11} what we wish to see is how this feature of $g(r)$ is related with the osmotic second virial coefficient. The $g(r)$ obtained here is so accurate that one can also see that the second and third peaks become higher and the second minimum becomes lower with decreasing temperature. This means that the calculation of B_{long} in eq 7 becomes important at low temperatures.

Figure 4 shows the osmotic second virial coefficient B as a function of temperature. Each point is the average of B in eq 7 over r_c from 12 to 20 Å. The error bars are the maximum and minimum values in the range of r_c . In the supercooled states of water at 238 and 258 K, it is found that $B > 0$, and so the net effective interaction between methane molecules in water is repulsive; around 273 K, $B \simeq 0$, i.e., the pair correlation is superficially null; and finally at higher temperatures $B < 0$, and so the net effective interaction is attractive. In the range of temperature between 238 and 373 K, B monotonically decreases from 63 to -81 cm³/mol with increasing temperature.

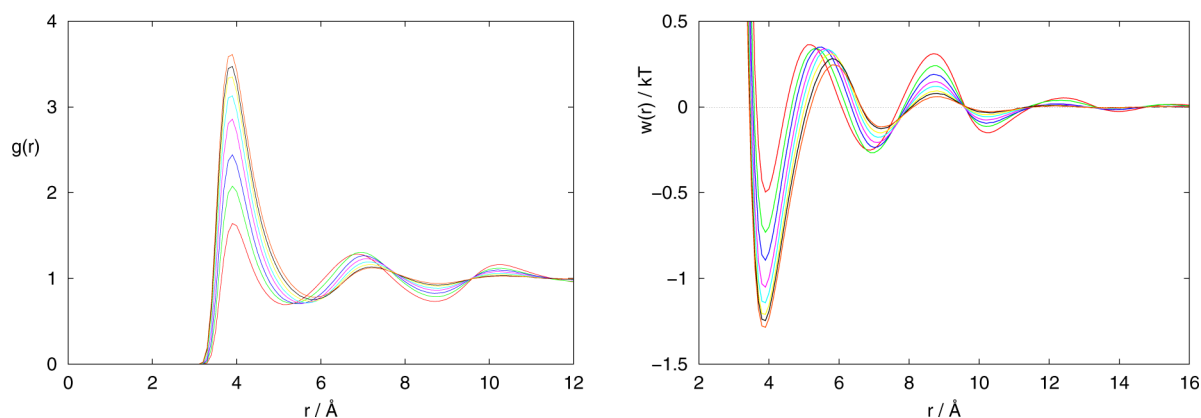


Figure 3. (a) The radial distribution function $g(r)$ and (b) the potential $w(r)$ of mean force for methane in water at 1 bar. The first peak of $g(r)$ rises and the first minimum of $w(r)$ decreases with increasing temperature in the order 238, 258, 278, 298, 318, 338, 358, and 373 K.

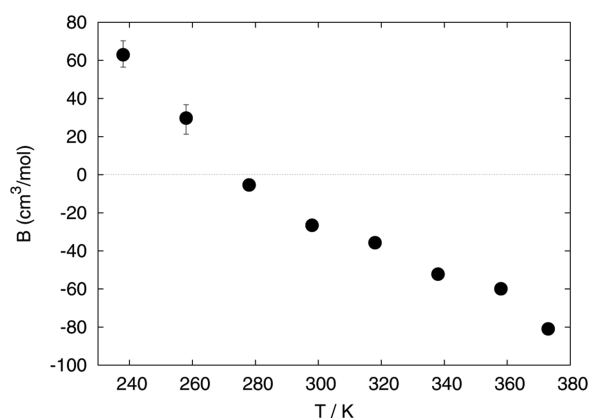


Figure 4. The osmotic second virial coefficient B for methane in water at 1 bar. The error bars indicate the maximum and minimum values of B as a function of r_c in eq 7 in the range $12 \text{ \AA} \leq r_c \leq 20 \text{ \AA}$: they are smaller than the circles at high temperatures.

There are several earlier results on B of methane in water: Watanabe and Anderson's estimate from solubility measurements of the gas is $B = -20 \text{ cm}^3/\text{mol}$ at 298 K;² Kennan and Pollack's results from the same thermodynamic formula with different experimental data are $B = 6.5$ or $-112 \text{ cm}^3/\text{mol}$;¹⁵ and Lüdemann et al. obtained $B = -16 \text{ cm}^3/\text{mol}$ at 300 K from the correlation-function integral over a finite distance.⁷ Our estimate from the full correlation-function integral (eq 7) is $B = -27 \text{ cm}^3/\text{mol}$ at 298 K.

We also note that B for methane at 298 K is of the same order of magnitude as our earlier estimate for propane ($-41 \text{ cm}^3/\text{mol}$) from the correlation-function integral,²⁰ but the former is less negative than the latter. There are two opposing reports on the solute-size dependence of B : B decreases with increasing molecular size of solute^{8,15} and its opposite.² Our results for methane and propane support the former.

In a dilute aqueous solution, if one cannot notice the solvent, one would find that methane molecules interact with each other via $w(r)$, the potential of mean force, instead of via the pair potential $\phi(r)$ in the gas phase, and so the osmotic B is equivalent to B_{gas} for molecules interacting with $w(r)$ in a vacuum. That is the conclusion of the McMillan–Mayer theory (eq 1). It may then be worth comparing B with B_{gas} in order to quantify the effect of the solvent on the pair potential. In Figure 5 are plotted B and B_{gas} together as functions of temperature. The curve is $B_{\text{gas}}(T)$ calculated for the model methane gas, and the three dots along the curve are experimental data. At 238 K, the lowest temperature examined, B and B_{gas} are of the same magnitude but their signs are opposite, and as T increases, the decreasing B and increasing B_{gas} cross each other at around 318 K with a value close to $-36 \text{ cm}^3/\text{mol}$, and then at 373 K, B (<0) becomes 4 times larger in magnitude than B_{gas} (<0), indicating that the hydrophobic attraction is indeed very strong at high temperatures.

We shall now examine the effect of the direct attractive potential $\phi_{\text{attr}}(r)$ between solute molecules, which is now $\phi(r) - \phi_{\text{WCA}}(r)$. The triangles in Figure 5 show the osmotic second virial coefficient B_{WCA} of the WCA solute particles. Note that $B_{\text{WCA}} > 0$ in the temperature range is larger than B for methane at any given temperature. This illustrates that the attractive part of the direct pair potential has a significant contribution to B . The difference is about $110 \text{ cm}^3/\text{mol}$ at any T ; i.e., $B(T)$ and $B_{\text{WCA}}(T)$ are nearly parallel to each other. One may then conclude that the effect of the direct attractive potential ϕ_{attr} on

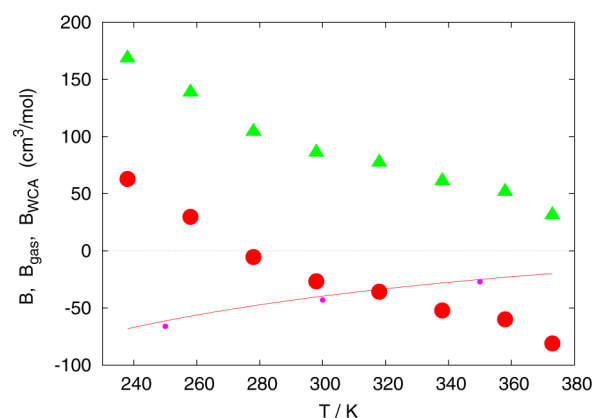


Figure 5. Comparison of B for methane in water (circles) with the second virial coefficient B_{gas} for methane (line, calculation; dots, experiment) and the osmotic B for the WCA solute particles in water (triangles). The error bars for B for methane and the WCA solute (not shown) are the same as those in Figure 4.

the temperature dependence of B is much smaller than the solvent-induced effect.

The difference $B_{\text{WCA}} - B \approx \text{cm}^3/\text{mol}$ comes solely from the difference in the solute–solute pair potential: $\phi(r) - \phi(r)_{\text{WCA}}$. The effect of solute–solvent attractive interaction is not examined here, but previous theoretical studies have already demonstrated that the weaker the attractive solute–solvent interaction the stronger the attractive solvent-induced interaction between solute molecules.^{1,4,14} Then, if the solute–solvent pair potential is also purely repulsive as the solute–solute potential, B_{WCA} would be less positive than it is now and could be negative in a wide range of temperatures. It is worth calculating B for such solutes as they are similar to cavities in water whose effective interactions have been studied by the information-theory model.^{12,13}

As illustrated above, to obtain B from $g(r)$, one must have $g(r)$ with significant accuracy up to large distances where the oscillations in $g(r)$ are vanishingly small. It would then be of great value if there is a simple relation between B and the first-peak height of $g(r)$, for the latter may be obtained easily and is a simpler measure of the effective attraction. The distance r_1 at which the first peak is found is $r_1 = 3.9 \text{ \AA}$ for all the temperatures and for the methane and WCA solutes. We saw that $g(r_1)$ increases and B decreases with increasing temperature, as shown in Figures 2 and 3, respectively, and as listed in Table 1. That is also true for the WCA solute in water. In Figure 6 are shown the plots of B against $g(r_1)$, both for methane in water and for the WCA solute in water. These are nearly linear over the temperature range, and for the two solute models are nearly parallel and close to each other. The linear relation between B and $g(r_1)$ for methane is

$$B/\sigma^3 = -2.15g(r_1) + 5.41 \quad (\text{methane}) \quad (8)$$

and that for the WCA solute is

$$B/\sigma^3 = -2.60g(r_1) + 7.41 \quad (\text{WCA}) \quad (9)$$

with $\sigma = 3.73 \text{ \AA}$, the LJ size parameter for the solute molecules.

IV. SUMMARY

A scheme for calculating the osmotic second virial coefficient B of small solute molecules in a solvent was proposed and applied to the model system of an aqueous solution of methane. The

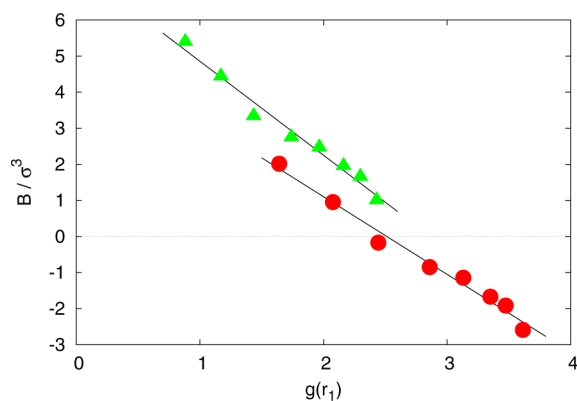


Figure 6. B against the first-peak height $g(r_1)$ for methane (circles) and that for the WCA solute (triangles). The lines are the least-squares fit to each set of the data.

full correlation-function integral (eq 2) is calculated as a sum of B_{short} and B_{long} , the short-range and long-range contributions to B , where B_{short} is calculated from an accurate infinite-dilute limit of $h(r)$ obtained by molecular dynamics simulation while B_{long} is from the exact asymptotic form of $h(r)$ derived by Evans et al.²⁷ It was shown that evaluation of B_{long} is important at low temperatures because then oscillations in $h(r)r^2$, which is to be integrated over r , are appreciable even at the largest distance accessible by the molecular simulation of an aqueous solution containing 4000 water molecules. It was demonstrated that B for methane in water is positive for supercooled water, zero around the freezing point, and negative at higher temperatures, as monotonically decreasing with increasing temperature. The osmotic B for methane in water is equal to B_{gas} for gaseous methane at around 320 K, below which $B > B_{\text{gas}}$ and above which $B < B_{\text{gas}}$. In this sense, the hydrophobic interaction is less attractive than the pair interaction of the gas at low temperatures and it is much more attractive than the gas-phase interaction near the boiling point of water. The osmotic B_{WCA} for the WCA solute particles, which have no direct attraction among them, is larger than B by about 110 cm³/mol, but the temperature dependences are nearly the same as that of B . Finally, it was found that the relation between B and $g(r_1)$, the first-peak height of the solute–solute radial distribution function, is nearly linear both for the methane solute and for the WCA solute. It would be of great value if validity of the linear relation is found for a large class of solutions.

AUTHOR INFORMATION

Notes

The authors declare no competing financial interest.

ACKNOWLEDGMENTS

The author thanks Ben Widom for discussions about the asymptotic, long-range behavior of the correlation functions and bringing the work by Bob Evans et al.²⁷ to my attention. The author acknowledges support by a Grant-in-Aid for Scientific Research and the Next Generation Super Computing Project from MEXT, Japan.

REFERENCES

- Pratt, L. R.; Chandler, D. Theory of The Hydrophobic Effect. *J. Chem. Phys.* **1997**, *67*, 3683–3704.
- Watanabe, K.; Andersen, H. C. Molecular Dynamics Study of The Hydrophobic Interaction in An Aqueous Solution of Krypton. *J. Phys. Chem.* **1986**, *90*, 795–802.
- Wood, R. H.; Thompson, P. T. Differences Between Pair and Bulk Hydrophobic Interactions. *Proc. Natl. Acad. Sci. U.S.A.* **1990**, *87*, 946–949.
- Smith, D. E.; Haymet, A. D. J. Free-Energy, Entropy, and Internal Energy of Hydrophobic Interactions - Computer-Simulations. *J. Chem. Phys.* **1993**, *98*, 6445–6454.
- Dang, L. X. Potential of mean force for the methane–methane pair in water. *J. Chem. Phys.* **1994**, *100*, 9032–9034.
- Rick, S. W.; Berne, B. J. Free Energy of The Hydrophobic Interaction from Molecular Dynamics Simulations: The Effects of Solute and Solvent Polarizability. *J. Phys. Chem. B* **1997**, *101*, 10488–10493.
- Lüdemann, S. L.; Abseher, R.; Schreiber, H.; Steinhauser, O. The Temperature-Dependence of Hydrophobic Association in Water. Pair versus Bulk Hydrophobic Interactions. *J. Am. Chem. Soc.* **1997**, *119*, 4206–4213.
- Liu, H.; Ruckenstein, E. Aggregation of Hydrocarbons in Dilute Aqueous Solutions. *J. Phys. Chem. B* **1998**, *102*, 1005–1012.
- Shimizu, S.; Chan, H. S. Temperature Dependence of Hydrophobic Interactions: A Mean Force Perspective, Effects of Water Density, and Nonadditivity of Thermodynamic Signatures. *J. Chem. Phys.* **2000**, *113*, 4683–4700.
- Matubayasi, N.; Nakahara, M. Association and Dissociation of Nonpolar Solutes in Super- and Subcritical Water. *J. Phys. Chem. B* **2000**, *104*, 10352–10358.
- Paschek, D. Temperature Dependence of The Hydrophobic Hydration and Interaction of Simple Solutes: An Examination of Five Popular Water Models. *J. Chem. Phys.* **2004**, *120*, 6674–6690.
- Hummer, G.; Garde, S.; García, A. E.; Pohorille, A.; Pratt, L. R. An Information Theory Model of Hydrophobic Interactions. *Proc. Natl. Acad. Sci. U.S.A.* **1996**, *93*, 8951–8955.
- Hummer, G. Hydrophobic Force Field as a Molecular Alternative to Surface-Area Models. *J. Am. Chem. Soc.* **1999**, *121*, 6299–6305.
- Asthağiri, D.; Merchant, S.; Pratt, L. R. Role of Attractive Methane–Water Interactions in The Potential of Mean Force between Methane Molecules in Water. *J. Chem. Phys.* **2008**, *128*, 244512-1–244512-7.
- Kennan, R. P.; Pollack, G. L. Pressure Dependence of The Solubility of Nitrogen, Argon, Krypton, and Xenon in Water. *J. Chem. Phys.* **1990**, *93*, 2724–2735.
- Widom, B.; Underwood, R. C. Second Osmotic Virial Coefficient from the 2-Component Van Der Waals Equation of State. *J. Phys. Chem. B* **2012**, *116*, 9492–9499.
- Widom, B.; Koga, K. Note on the Calculation of the Second Osmotic Virial Coefficient in Stable and Metastable Liquid States. *J. Phys. Chem. B* **2013**, *117*, 1151–1154.
- McMillan, W. G.; Mayer, J. E. The Statistical Thermodynamics of Multicomponent Systems. *J. Chem. Phys.* **1945**, *13*, 276–305.
- Kirkwood, J. G.; Buff, F. P. The Statistical Mechanics Theory of Solutions. I. *J. Chem. Phys.* **1951**, *19*, 774–777.
- Koga, K.; Widom, B. Thermodynamic Functions as Correlation-Function Integrals. *J. Chem. Phys.* **2013**, *138*, 114504-1–114504-8.
- Abascal, J. L. F.; Vega, C. A General Purpose Model for The Condensed Phases of Water: Tip4p/2005. *J. Chem. Phys.* **2005**, *123*, 234505-1–234505-12.
- Hirschfelder, J. O.; Curtiss, C. F.; Bird, R. B. *Molecular Theory of Gases and Liquids*; Wiley: New York, 1954.
- Docherty, H.; Galindo, A.; Vega, C.; Sanz, E. A Potential Model for Methane in Water Describing Correctly The Solubility of The Gas and The Properties of The Methane Hydrate. *J. Chem. Phys.* **2006**, *125*, 074510-1–074510-9.
- Young, W. S.; Brooks, C. L., III. A Reexamination of The Hydrophobic Effect: Exploring The Role of The Solvent Model in Computing The Methane–Methane Potential of Mean Force. *J. Chem. Phys.* **1997**, *106*, 9265–9269.

(25) Lebowitz, J. L.; Percus, J. K. Long-Range Correlations in A Closed System with Applications to Nonuniform Fluids. *Phys. Rev.* **1961**, *122*, 1675–1691.

(26) Kežić, B.; Perera, A. Aqueous Tert-Butanol Mixtures: A Model for Molecular-Emulsions. *J. Chem. Phys.* **2012**, *137*, 014501-1–014501-12.

(27) Evans, R.; de Carvalho, R. J. F. L.; Henderson, J. R.; Hoyle, D. C. Asymptotic Decay of Correlations in Liquids and Their Mixtures. *J. Chem. Phys.* **1994**, *100*, 591–603.

(28) Hess, B.; Kutzner, C.; van der Spoel, D.; Lindahl, E. GROMACS 4: Algorithms for Highly Efficient, Load-Balanced, and Scalable Molecular Simulation. *J. Chem. Theory Comput.* **2008**, *4*, 435–447.